



Contents lists available at ScienceDirect

Physics Letters A

www.elsevier.com/locate/pla

Large negative differential resistance in graphene nanoribbon superlattices

P. Tseng, C.H. Chen, S.A. Hsu, W.J. Hsueh*

Nanomagnetism Group, Department of Engineering Science and Ocean Engineering, National Taiwan University, 1, Sec. 4, Roosevelt Road, Taipei, 10660, Taiwan

ARTICLE INFO

Article history:

Received 31 October 2017

Received in revised form 19 March 2018

Accepted 26 March 2018

Available online xxxx

Communicated by M. Wu

Keywords:

Electronic transport in graphene

Negative differential resistance

Structure and nanoelectronic properties of superlattices

Band structure

ABSTRACT

A graphene nanoribbon superlattice with a large negative differential resistance (NDR) is proposed. Our results show that the peak-to-valley ratio (PVR) of the graphene superlattices can reach 21 at room temperature with bias voltages between 90–220 mV, which is quite large compared with the one of traditional graphene-based devices. It is found that the NDR is strongly influenced by the thicknesses of the potential barrier. Therefore, the NDR effect can be optimized by designing a proper barrier thickness. The large NDR effect can be attributed to the splitting of the gap in transmission spectrum (segment of Wannier–Stark ladder) with larger thicknesses of barrier when the applied voltage increases.

© 2018 Elsevier B.V. All rights reserved.

1. Introduction

Since the discovery of negative differential resistance (NDR) in an Esaki tunneling diode [1], it has been applied to design numerous devices such as high frequency oscillators, memory cells, and multiple-valued logic [2–5]. In addition to Esaki tunneling diodes, NDR has also been observed in various systems, including carbon nanotubes [6] and Fullerene-C₆₀ [7]. Recently, graphene has attracted much interest because graphene-based devices exhibit may have better performance than their semiconductor counterparts in terms of speed and power consumption [8–10]. This result is the consequence of the unique properties of graphene, such as high mobility of carriers, which provides high current densities. NDR has also been investigated in graphene-based devices, such as monolayer graphene [11–15], bilayer graphene [16,17], graphene nanoribbons [18], and graphene tunnel diodes [19]. However, compared with the traditional semiconductor-based NDR devices, the peak-to-valley ratios (PVR) of NDR in two-dimensional graphene-based devices are ordinary.

The concept of a superlattice, which is a man-made material that consists of alternating layers of two dissimilar materials with layer thicknesses in the order of nanometers, has been used in

phononics [20–23], spintronics [24–29], and electronics [30–32]. One of the most important advantages of a superlattice is its flexibility compared with a natural material [33]. Recent studies suggested that the electronic behaviors of massless Dirac fermions in graphene have been predicted by applying external period potentials [34,35] and high PVR devices have been reported in experiment [36,37]. Therefore, it is an interesting topic to improve the NDR of graphene-based devices by using the concept of a superlattice. To the best of our knowledge, only a fraction of studies have focused on various important applications of NDR by combining the unusual characteristics of superlattices with graphene. Although extraordinary NDR effect at low temperature in graphene superlattices have been proposed by doping [38] or top gate voltage [39], the performance of the NDR in those devices at room temperature are usually limited. The reason is that the Fermi–Dirac distribution also strongly influences NDR in the current. In addition, there are many flexible operations of nanostructured graphene in the entire system due to the tunable potential by metal electrodes on graphene [40]. In this paper, the PVR of the NDR in a 7-cell graphene superlattice can be optimized up to 21 at room temperature, provided that the barrier/well thickness of the graphene superlattice is properly designed. The significant NDR effect is observed in wide thicknesses of barrier and a large number of cells. The physical mechanism will also be explained by both the transmission spectrum and Fermi–Dirac distribution.

* Corresponding author.

E-mail address: hsuehwj@ntu.edu.tw (W.J. Hsueh).

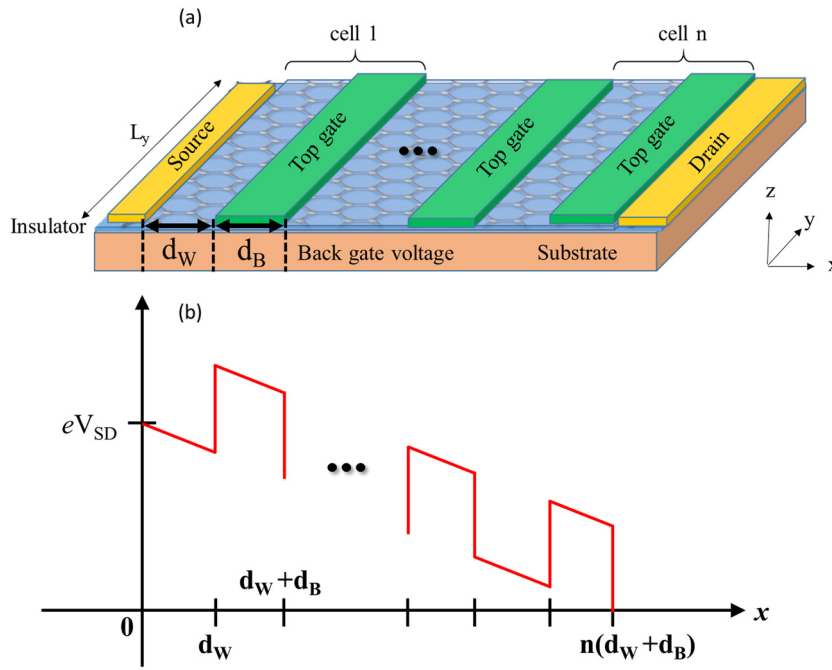


Fig. 1. (a) Upper panel shows the monolayer graphene nanoribbon embedded in insulator and substrate, with n-strips of electrode on top of the insulator. These strips of electrode and substrate are applied with the top gate voltage and back gate voltage respectively. The graphene nanoribbon is connected to source and drain leads, resulting in biased transport under source-drain voltage, V_{SD} . The corresponding potential profiles of the unbiased device are shown in the lower panel. (b) Potential profiles for the three-barrier superlattice with source-drain voltage $V_{SD} = 600$ mV.

2. Model and formulation

An n-barrier armchair graphene nanoribbon (AGNR) superlattice is shown in Fig. 1(a). The monolayer graphene nanoribbon is embedded in an insulator and substrate, with n-strips of electrode on top of the insulator. These strips of electrode and substrate are applied with the top gate voltage and back gate voltage, respectively. The top gate voltage is 230 mV throughout this paper. The AGNR superlattice is further connected to source and drain leads, resulting in biased transport under source-drain voltage, V_{SD} . The chemical potential can be adjusted by the back gate voltage, thereby setting the chemical potential for $\mu = eV_G$. This model requires the graphene nanoribbon to be ultraclean and ultrasmooth, and the edge effect can be neglected. Moreover, the electrode contact is idealized, and the voltages drop linearly along the sample. Fig. 1(b) shows the potential profile of a n-cell AGNR superlattice. The potential profile is $eV_j = U_j - eV_{SD}(\frac{x_j}{L})$ where x_j is the center coordinate of j th layer, and L is the length of the device between source and drain leads. The width of the barrier and well are denoted by d_B and d_W , respectively. The low-energy electronic state of graphene can be calculated by the Dirac equation [41]. The Hamiltonian for carriers near the Dirac points $K = (4\pi/3a, 0)$ and $K' = (-4\pi/3a, 0)$ can be expressed as

$$H = v_F \begin{pmatrix} U(x) & p_x \mp ip_y \\ p_x \pm ip_y & U(x) \end{pmatrix}, \tag{1}$$

where $p_x = -i\hbar \frac{\partial}{\partial x}$ and $p_y = -i\hbar \frac{\partial}{\partial y}$ are the momentum operators, $U(x)$ is the potential barrier by the top gate voltage, and v_F is the Fermi velocity. The system investigated in this study is homogeneous along the y direction. To solve the Dirac Hamiltonian $H\Psi = E\Psi$, the eigenvector is given by a state of two-component pseudospinor $\Psi = (\psi_A, \psi_B)^T$. The detailed formulas of eigenvector inside the j th potential can be expressed as

$$\Psi_j = \left\{ A_j \begin{pmatrix} 1 \\ e^{i\theta_j} \end{pmatrix} e^{iq_{x,j} \cdot x} + B_j \begin{pmatrix} 1 \\ -e^{-i\theta_j} \end{pmatrix} e^{-iq_{x,j} \cdot x} \right\} e^{iky \cdot y}, \tag{2}$$

where the subscript j denotes each element in the j th segment, A_j and B_j are the amplitude coefficients of incident and reflected waves, respectively, $\cos \theta_j = q_{x,j}/k_j$, $k_j = (E - U_j)/\hbar v_F$, k_y is the y component of the wave vector, and $q_{x,j}$ is the x component of the wave vector, which is $q_{x,j} = \text{sign}(k_j) \sqrt{k_j^2 - k_y^2}$ for $k_j^2 > k_y^2$ and $q_{x,j} = i \sqrt{k_y^2 - k_j^2}$ for $k_j^2 < k_y^2$. The boundary conditions at the edges of an AGNR lead to the quantization of the transverse wave vector. For semiconducting AGNRs, the allowed transverse wave vector $|k_{y,m}| = m\pi/3L_y$, where $m = 1, 2, 4, 5, 7, 8, \dots$. The resulting half-bandgap is obtained by $E_0 = \pi \hbar v_F / 3L_y$ [42]. The transverse momentum k_y is conserved because the potentials depend only on the longitudinal coordinate.

Based on the boundary conditions and the transport model of electron, the relation of amplitude coefficients for incident and reflected waves between the neighbor layers is

$$\begin{Bmatrix} A_{j+1} \\ B_{j+1} \end{Bmatrix} = (P_{j+1})^{-1} F_j \begin{Bmatrix} A_j \\ B_j \end{Bmatrix}, \tag{3}$$

where $F_j = M_j P_j$, $M_j = \begin{pmatrix} e^{iq_{x,j} \cdot d_j} & e^{-iq_{x,j} \cdot d_j} \\ e^{i(q_{x,j} \cdot d_j + \theta_j)} & -e^{-i(\theta_j + q_{x,j} \cdot d_j)} \end{pmatrix}$, and $P_j = \begin{pmatrix} 1 & 1 \\ e^{i\theta_j} & -e^{-i\theta_j} \end{pmatrix}$. Therefore, the total transfer matrix in the entire system is written as

$$\begin{Bmatrix} A_D \\ B_D \end{Bmatrix} = H_t \begin{Bmatrix} A_S \\ B_S \end{Bmatrix}, \tag{4}$$

where the total transfer matrix H_t is given by

$$H_t = P_D^{-1} \left(\prod_{j=1}^n M_j P_j^{-1} \right) P_S. \tag{5}$$

Download English Version:

<https://daneshyari.com/en/article/8203440>

Download Persian Version:

<https://daneshyari.com/article/8203440>

[Daneshyari.com](https://daneshyari.com)